Counterpropagating Fractional Hall States in Mirror-Symmetric Dirac Semimetals

Yafis Barlas

Phys. Rev. Lett. **121**, 066602 — Published 7 August 2018

DOI: 10.1103/PhysRevLett.121.066602

Counter-propagating Fractional Hall states in mirror-symmetric Dirac semi-metals

Yafis Barlas[1]

[1] *Department of Electrical and Computer Engineering, University of California, Riverside, California**

The Landau bands of mirror symmetric 2D Dirac semi-metals (for example odd-layers of ABA-graphene) can be identified by their parity with respect to mirror symmetry. This symmetry facilitates a new class of counter-propagating Hall states. We predict the presence of a Laughlin-like correlated liquid state, at the charge neutrality point, with opposite but equal electron and hole filling factors $|\nu_{\pm}| = 1/m$ (m odd). This state exhibits fractionally charged quasi-particle/hole pair excitations and counter-propagating edge states with opposite parity. Using a bosonized one-dimensional edge state theory, we show that the fractionally quantized two-terminal longitudinal conductance, $\sigma_{xx} = 2e^2/(mh)$, is robust to short-ranged inter-mode interactions.

The quantum spin Hall (QSH) state [1, 2], is characterized by one-dimensional helical edge states. This results in a quantized longitudinal two-terminal resistance [3] along with a vanishing Hall resistance. Time reversal symmetry in the QSH state is essential, as it forbids back-scattering of the helical edge modes. Such symmetry protected topological (SPT) states can also be realized in Dirac semi-metals (graphene and bilayer graphene) at neutral charge density in the quantum Hall (QH) regime. Interactions in the $\nu = 0$ QH state in graphene and bilayer graphene result in an insulating canted antiferromagnetic (CAF) state [4], due to spontaneous ordering of the half-filled spin and valley degenerate Landau level. As the in-plane magnetic field is increased, this insulating CAF state transitions to a ferromagnetic state with counter-propagating spin polarized edge modes and a quantized two-terminal conductance [4–6]. Here, the robust quantization requires spin rotational symmetry. Other interaction induced symmetry protected topological (SPT) states, like fractional topological insulators [7] have also been proposed, but not realized experimentally. In this Letter, we propose a new class of interacting and non-interacting SPT phases protected by mirror symmetry in 2D Dirac semi-metals.

In 2D Dirac semi-metals, Fermi-surface (FS) topology at neutral charge density can lead to two distinct types of semi-metallic band structures. Since the conduction band minima and valance band maxima must coincide in momentum space, this gives only two distinct possibilities for FS topology. At the charge neutrality point (CNP), either i) the FS consists of singular points in the Brillouin zone (BZ) (for example graphene and bilayer graphene bands), or ii) non-zero electron and hole pockets with, $n_e = -n_h$, co-exist at neutral charge density. The latter FS topology is only robust to perturbations, if the spinless electron and hole pockets belong to different irreducible representations of the lattice symmetry. The second scenario can be viewed as the analogue of band inversion in Dirac semi-metals. It is satisfied in the ABA-stacked trilayer graphene [8, 9].

Layered graphene stacks, held together by van der Waals forces, add an extra degree of richness to graphene's electronic properties [10–12]. One such stacking configuration is the ABA-stacked multilayer graphene. In this configuration, each layer has the same in-plane projection as its next nearest neighboring layer, implying that all next nearest layers are exactly aligned but vertically displaced. Additionally, each nearest neighboring layer is Bernal stacked, such that half of the atoms in alternate layers lie directly over the center of the hexagon while the other half lie directly over the atom in the nearest neighboring layer (see Fig. 1 (a) & (b)). It follows that the even and odd layer stacks belong to different symmetry groups. Even N-layer ABA-multilayer graphene stacks are inversion symmetric (i.e. $\vec{r} \to -\vec{r}$), whereas odd N-layer ABA-multilayer graphene stacks satisfy mirror reflection symmetry (i.e. $(x, y, z) \to (x, y, -z)$). Therefore, the energy

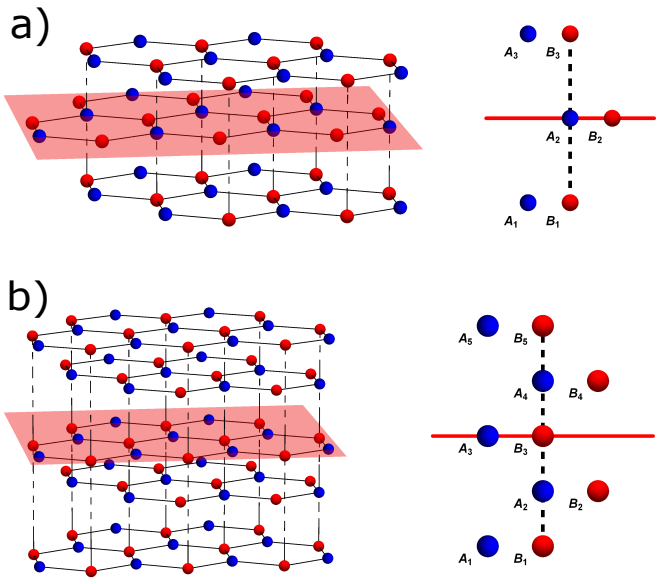

FIG. 1. Lattice structure of ABA-trilayer graphene (TLG) (a) and ABA-pentalayer graphene (b) with mirror symmetry about the middle layer denoted by the red line (plane). Under mirror symmetry $A_1 \leftrightarrow A_3$, $B_1 \leftrightarrow B_3$, whereas the middle layer remains invariant for ABA-TLG.

bands of odd N-layer graphene sheets can be classified in terms of their parity ($\eta = \pm$) with respect to mirror reflection [9]. Furthermore, because of this lattice symmetry, the Hamiltonian of odd N-layer ABA-multilayer graphene becomes block diagonal in terms of the parity eigenstates.

To make the discussion more precise, consider the simplest mirror symmetric 2D Dirac semi-metal: ABA-trilayer graphene (TLG). ABA-TLG is invariant under the D_{3h} point group, which includes mirror symmetry about the middle layer. From now on we denote the inequivalent atomic sites of the i^{th} graphene layer by A_i and B_i. The lattice stacking is such that only half of the sub-lattice sites in each layer (B_1, A_2, B_3) have a near-neighbor in the adjacent layer, whereas the other half (A_1, B_2, A_3) don't have a near neighbor in the adjacent layers (see Fig. 1 a). Under mirror symmetry the sub-lattices on the top layer are interchanged with the sub-lattices in the bottom layer, $\psi_{A_1} \leftrightarrow \psi_{A_3}$ and $\psi_{B_1} \leftrightarrow \psi_{B_3}$, whereas the sub-lattices of the middle layer remain unchanged, $\psi_{A_2} \leftrightarrow \psi_{A_2}$ and $\psi_{B_2} \leftrightarrow \psi_{B_2}$.

In general, the mirror symmetry operator $\mathcal{M}$ can be expressed as a rotation by π with the axis of rotation perpendicular to the mirror plane, followed by an inversion. This gives $\mathcal{M} = PD(\pi)$, where P is the inversion operator which sends $\vec{r} \to -\vec{r}$, and $D(\pi)$ is the rotation operator which acts on the internal degrees of freedom such as spin. For spinless particles, this rotation matrix acts trivially and is equal to the identity matrix. The mirror symmetry operator satisfies $\mathcal{M}^2 = 1$ with eigenvalues ± 1, corresponding to the even and odd parity. For ABA-TLG the sub-lattice orbital combinations $A_\pm = (A_1 \pm A_3)/\sqrt{2}$ and $B_\pm = (B_1 \pm B_3)/\sqrt{2}$, form the irreducible representations of this mirror symmetry. $A_\pm$ and $B_\pm$ have $+(-)$ even (odd) parity with respect to this mirror symmetry, while the middle layer A_2 and B_2 orbitals have even parity [10, 13].

Therefore, the Hamiltonian for ABA-TLG can be separated into contributions from even and odd parity Hamiltonians, $\mathcal{H} = \mathcal{H}_- \otimes \mathcal{H}_+$ [13]. The energy bands of the odd parity orbitals (A_-, B_-) belong to the class of gapped Dirac-like dispersion with,

$$\mathcal{H}_- = \hbar v(\hat{\sigma}_x \pi_x + \tau_z \hat{\sigma}_y \pi_y) + m_- \hat{\sigma}_z + \frac{\Delta}{2}\hat{\sigma}_0, \qquad (1)$$

where σ_i's denote the Pauli matrices and $\sigma_0 = \mathbb{I}_2$. Eq. (1) is acts on the odd-parity spinors, $\psi^\dagger_{o,\tau} = (\phi^\dagger_{A_-,\tau}, \phi^\dagger_{B_-,\tau})$, $\tau = \pm$ denotes the $\mathbf{K}(\mathbf{K}')$ valley in the hexagonal BZ, $\hbar v = 688$ meV nm, $\pi_i = i\partial_i - eA_i$ is the momentum operator in a high magnetic field $B\hat{z} = \nabla \times A$, satisfying $[\pi_x, \pi_y] = -i/l_B^2$, where $l_B = \sqrt{\hbar/eB}$ is the magnetic length. The mass gaps $\Delta = 27$ meV and $m_- = 3$ meV are determined by the remote inter-layer hopping parameters and energy differences between stacked and non-stacked atoms [14].

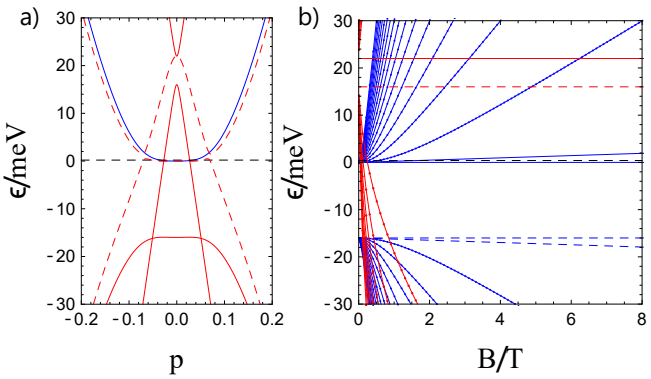

FIG. 2. a) Energy dispersion of ABA-TLG at $E_\perp = 0$ (solid line) and $E_\perp = 40$meV (dashed line). The semi-metallic phase requires $|\Delta| > (m_+ + m_-)$. (b) Landau level spectrum of ABA-TLG. In both figures red represents the odd parity electrons and blue denotes the even parity electrons and the black dotted line denotes the Fermi energy at the CNP. The dotted and solid lines denote different valleys (sub-lattices for the zLLs). At neutral charge density ($\nu = 0$) the even parity filling factor is $\nu_+ = 2$, while the odd parity filling factor is $\nu_- = -2$.

The even parity orbitals (A_+, B_2, A_2, B_+), exhibit a band dispersion similar to gapped bilayer graphene. At low-energies the orbitals A_2 and B_+ are pushed to high energies due to the direct inter-layer hopping $\gamma_1 \sim 0.31$ eV. The resulting low-energy even parity Hamiltonian [15], $\mathcal{H}_+$ acts on the even-parity spinors $\psi^\dagger_{e,\tau} = (\phi^\dagger_{A_+,\tau}, \phi^\dagger_{B_2,\tau})$ [13],

$$\mathcal{H}_+ = \frac{-\hbar^2 v^2}{\sqrt{2}\gamma_1}\left(\hat{\sigma}_x(\pi_x^2 - \pi_y^2) + \tau_z \hat{\sigma}_y\{\pi_x, \pi_y\}\right) + m_+\hat{\sigma}_z - \frac{\Delta}{2}\hat{\sigma}_0, \qquad (2)$$

here $\{...\}$ denotes the anti-commutator with $m_+ = 8$ meV [14]. To ensure the semi-metallic FS topology (see in Fig 2 a), electron-hole band overlap at the CNP requires $|\Delta| > (m_- + m_+)$ at zero displacement field, $E_\perp = 0$.

The LL spectrum of ABA-TLG, plotted in Fig 2 b, shows that only the energies of the zeroth ($N = 0$) LLs, are magnetic field independent [13, 14]. The odd and even parity zLLs, including the spin and valley degeneracy, have four and eight flavor components respectively. A common feature of $\mathcal{H}_+$ is the additional degeneracy associated with the $n = 0, 1$ LL orbitals in the even parity zLLs [16]. These even-parity zLL orbitals are further split by $\Delta_{LL} \sim 0.24B$ meV [17]. Additionally, lack of inversion symmetry in ABA-TLG breaks the valley degeneracy. The valley splitting is determined by the mass terms $m_+(m_-)$, for the even and odd parity zLLs, respectively. Due to the energy gap, $\tilde{\Delta} = \Delta - (m_+ + m_-) > 0$, the odd-parity zLLs (denoted by red) lie above the even-parity zLLs (denoted by blue).

The FS topology of ABA-TLG at the CNP (defined as $\nu = \nu_+ + \nu_- = 0$) implies that above a very weak

critical magnetic field $\nu_- = -2$ and $\nu_+ = +2$ (including spin degeneracy), where ν_η denotes the filling factor of the η-parity zLLs). The edge states associated with the even-parity electron and odd-parity hole-zLLs flow in opposite directions, as depicted in Fig. 3 (a) & (b). The counter-propagating edges modes at $\nu = 0$ are associated definite parity, which we call this the parity Hall effect. One consequence of this state is that $\sigma_{xy} = 0$ along with a quantized two-terminal longitudinal conductivity $\sigma_{xx} = 4e^2/h$. Mirror symmetry prohibits back-scattering of the counter-propagating even and odd parity branches ensuring the quantization of σ_{xx}. This phase and its broken symmetry counterparts have been detected in dual-gate ABA-TLG samples [18].

To proceed further, it is advantageous to express the zLL wavefunctions in the charge conjugation basis. Charge conjugation symmetry is defined as,

$$C_\eta^\dagger \mathcal{H}_\eta^\star(e) C_\eta = -\mathcal{H}_\eta(-e), \tag{3}$$

where C_η the charge conjugation symmetry operator is a unitary matrix, and e is the electron charge. It is easy to verify that for the odd parity Hamiltonian $\mathcal{H}_-$, the charge conjugation operator is: $C_- = \hat{\sigma}_y \hat{\sigma}_z$, while for the even parity Hamiltonian $\mathcal{H}_+$, the charge conjugation operator is: $C_+ = \hat{\sigma}_y$. So as long as the mirror symmetry is preserved, $[\mathcal{M}, C_\eta] = 0$. One consequence of Eq. 3 is that, if $|\psi\rangle$ is an eigenstate of $\mathcal{H}_\eta$ with an eigenvalue E_η and charge e, then $C_\eta|\psi\rangle^\star$ is also an eigenstate with the eigenvalue $-E_\eta$ and charge $-e$. As we see below, this charge conjugation symmetry provides a natural basis for the many-body wavefunctions in the parity Hall state.

In the symmetric gauge, $\boldsymbol{A} = B/2(-y, x, 0)$, the even parity $n = 0$ orbital zLL electron-like and hole-like states in the charge conjugation basis become,

$$\langle z|l, +, B_2\rangle = z^l e^{-\frac{1}{4}|z|^2}, \quad \langle z|l, +, A_+\rangle = (z^\star)^l e^{-\frac{1}{4}|z|^2}, \tag{4}$$

where the electron-like states is localized on B_2 and the hole-like state is localized on A_+, $z = (x_+ + iy_+)/l_B$ denotes the position of the even parity electrons and l is the angular momentum quantum number. The hole-like state in Eq. 4 is calculated by applying C_+ to the conjugate of the even parity electron-like zLL wavefunction: $|l, +, B_2\rangle^\star$. Similarly, the odd-parity zLL hole-like and electron-like wavefunctions can be expressed as,

$$\langle w|l, -, A_-\rangle = (w^\star)^l e^{-\frac{1}{4}|w|^2}, \quad \langle w|l, -, B_-\rangle = w^l e^{-\frac{1}{4}|w|^2}, \tag{5}$$

which resides purely on the orbital A_- and B_- orbitals respectively, $w = (x_- + iy_-)/l_B$ denotes the position of the odd parity electrons.

The holomorphic and anti-holomorphic nature of the even and odd parity zLL lead to a Laughlin like class of correlated states [2], with fractional filling $|\nu_\pm| = 1/m(m$ odd) at the CNP ($\nu = \nu_+ + \nu_- = 0$),

$$\Psi_0 = \prod_{i<j}(z_i - z_j)^m (w_i^\star - w_j^\star)^m \prod_k e^{-\frac{1}{4}(|z_k|^2 + |w_k|^2)}. \tag{6}$$

The correlated wavefunction above satisfies mirror symmetry at $\nu = 0$, which requires invariance under $z_i \leftrightarrow w_i^\star$. The elementary excitations of Ψ_0, consists of a pair of quasi-electron/hole within each parity sector with fractional charge $e_\pm^\star = \nu_\pm e$ [19]. These excitations can be created by introducing an infinitesimal unit flux quanta at the position x_0 [19] with $\prod_i (z_i - x_0)(w_i^\star - x_0)\Psi_0$.

Ψ_0 is the zero-energy eigenstate of the model Hamiltonian, $H = V_{l,\eta} P_{i,j}^{\eta,i}$ with $l = (m-1)/2$, where $V_{l,\eta}$ is the well-known Haldane pseudo-potential and $P_{i,j}^{\eta,l}$ is the projection operator on relative angular momentum l, for $\eta = \pm$ parity zLL [20, 21]. This model Hamiltonian will coincide with the effective Hamiltonian at partial fillings as interactions, given by the energy scale $e^2/\epsilon l_B \sim (54/\epsilon)\sqrt{B}$ meV, renormalize the single-particle gap $\tilde{\Delta}$ [22]. In this case, the interaction induced gap, Δ_{e-e} can be estimated from previous studies of the fractional quantum Hall effect in graphene, for the $\nu = 1/3$ state $\Delta_{e-e} \sim 0.035 e^2/\epsilon l_B = (1.9/\epsilon)\sqrt{B}$ meV [23]. The phase diagram for the fractional parity Hall effect and the hierarchy of counter-propagating fractional states will be discussed elsewhere [24].

The topological properties and excitations can be captured by the effective theory of the fractional parity Hall effect. It can be derived by performing the duality transformation [25] on the Chern-Simons Landau Ginzburg (CSLG) action [26–28] describing the charge conjugate Laughlin state Ψ_0 (see supplemental section). The field theory is described by the effective Lagrangian,

$$\mathcal{L} = -\eta e \epsilon^{\mu\nu\rho} A_\mu \partial_\nu b_\rho^\eta - \eta e \theta_\eta \phi_0 \epsilon^{\mu\nu\rho} b_\mu^\eta \partial_\nu b_\rho^\eta - J_\mu^\eta j_\mu^\eta + \cdots, \tag{7}$$

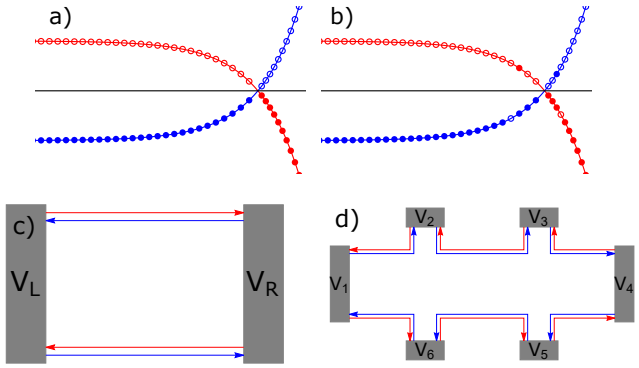

FIG. 3. a) and b) Edge dispersion of the $\nu = 1 + (-1)$ fractional parity Hall state, the counter-propagating edge currents flows due to particle-hole fluctuations in the even (blue) and odd (red) parity zLLs. Counter-propagating edge states of the fractional parity Hall effect in the two-terminal c) and Hall bar d) measurement setup.

where $\nu = 0, 1, 2$, $\eta = \pm$ and Einstein's summation convention is implied. The gauge fields b_μ and A_μ denote to the Chern Simons (CS) statistical and electromagnetic gauge fields, $\theta_\eta = \eta m\pi$ is the parameter angle related to the individual filling factor $|\nu_\pm|$ and $\phi_0 = hc/e$ is the flux quantum. The even and odd quasiparticle currents, given by j^μ_η, couple to the CS gauge field current $J^\eta_\nu = 2\pi b^\eta_\mu$, carry fractional charge $e^\star_\pm = \nu_\pm e$ and obey fractional statistics. The ground state degeneracy of $\mathcal{L}$ on a closed surface of genus g is $m^g \times m^g$, due to the contribution from each parity sector [29]. In Eq. 7, mirror symmetry at $\nu = 0$, given by $b_\eta \to b_{-\eta}$ and $\eta \to -\eta$, implies that $\sigma_{xy} = 0$. However, as we show below the fractional parity Hall state exhibits a fractionally quantized two-terminal longitudinal conductance.

Now, we turn to the question of the precise longitudinal quantization of the charge conjugate Laughlin state. For the non-interacting $m = 1$ charge conjugate Laughlin state, the edge excitations can be described in terms of single particle-hole excitations of the edge modes (see Fig. 3. The edge excitations consist of one-dimensional counter-propagating even and odd parity electron modes. In the presence of interactions, and for $m > 1$ this single-particle description fails and the edge states must be defined as one dimensional bosonic density excitations [30] along the edge. In terms of the bosonic field ϕ_η, the imaginary time action of the edge modes for Ψ_0 is given by,

$$S_0 = \frac{1}{4\pi|\nu_\pm|}\sum_{\eta=e,o}\int dxd\tau\partial_x\phi_\eta(i\eta\partial_\tau + v\partial_x)\phi_\eta, \qquad (8)$$

where the edge charge density is given by $\rho_\eta(x) = 1/(2\pi)\partial_x\phi_\eta$. The first terms encodes the Kac-Moody commutation relations $[\phi_\eta(x), \phi_{\eta'}(x')] = i\pi\nu_\eta sgn(x - x')\delta_{\eta,\eta'}$. We assume the velocity parameter v, determined by the intra-edge interactions and edge potential, is the same for both edge modes. Short-ranged inter-edge interactions, which can be expressed as,

$$S_{int} = \frac{v_d}{2\pi|\nu_\pm|}\int dxd\tau\partial_x\phi_e\partial_x\phi_o, \qquad (9)$$

result in equilibration of the edge modes. Their effect can be captured by diagonalizing the action $S = S_0 + S_{int}$. This is done by introducing chiral bosonic fields, $\varphi_{L(R)} = a_\mp\phi_e + a_\pm\phi_o$ with $a_\pm = (\gamma \pm 1)/(2\sqrt{\gamma})$ where $\gamma = \sqrt{v_+/v_-}$ and $v_\pm = v \pm v_d$. In terms of the chiral fields $\varphi_{L(R)}$ the bosonized imaginary time action becomes,

$$S = \frac{1}{4\pi|\nu_\pm|}\sum_{\alpha=L(R)}\int dxd\tau\big[\partial_x\varphi_\alpha(isgn(\alpha)\partial_\tau + u\partial_x)\varphi_\alpha\big] \qquad (10)$$

where $u = \sqrt{v_+v_-} = \sqrt{v^2 - v_d^2}$ and $sgn(\alpha) = \pm$ for the $R(L)$ chiral fields. In terms of the chiral fields the edge modes of Ψ_0 are just two decoupled chiral Luttinger liquids [31].

The one dimensional edge current is obtained from continuity equation, $I_{L(R)} = \dot{\varphi}_{L(R)}/(2\pi)$. When coupled to the electric potential $S \to S + \int dxd\tau\rho(x)V$, the transport characteristics of S can be calculated in linear response [31]. Consider the chiral edge modes flowing between two-reservoirs at different chemical potentials, as indicated in Fig. 3 (c). Using the Kubo formula for conductivity the current flowing along the top is given by, $I_t = g(V_1 - V_2)$ and at the bottom $I_b = g(V_2 - V_1)$ with $g = |\nu_\pm|e^2/h$. This gives the net current,

$$I = I_t - I_b = 2|\nu_\pm|\frac{e^2}{h}(V_L - V_R), \qquad (11)$$

resulting in two-terminal conductance $G = 2|\nu_\pm|e^2/h$, independent of the velocity. It is then straightforward to generalize the above results to calculate the resistance in a Hall bar geometry, see Fig. 3 (d). Using the multi-terminal Landuer-Buttiker theory for a Hall bar geometry, with a voltage applied between leads 1 and 4, we find zero Hall resistance, $R_{14,26} = 0$, and a fractionally quantized longitudinal resistance, $R_{14,14} = h/(2|\nu_\pm|e^2)$.

The effect of random edge disorder can be characterized by a localization length. This localization length has a power-law dependence on the strength of the disorder [31]. It determines the sample dimensions for which the quantized longitudinal conductivity can be observed. If the distance between the leads in Fig. 3 is smaller than the localization length, the system will be equivalent to a disorder-free system and the conductance will be given by (11). For rough edges, sharp local gates can be used to move the physical edge inside the sample thus preserving the requirement of mirror symmetry along the sample edges.

The fractional parity Hall states proposed here can be detected in Hall measurements. With the chemical potential pinned to the charge neutrality point, the individual filling factors $\nu_\pm = 2\pi n_\pm l_B^2 \propto 1/B$ can be modified by increasing the magnetic field. As the field is increased, plateaus in the longitudinal conductivity at $2|\nu_\pm|e^2/h$ should appear at certain fractional fillings $|\nu_\pm| = 1/m$ in each parity sector, for sufficiently clean samples. Since the parity Hall states require mirror symmetry they are gate tunable. At other partial fillings, exchange interactions will lead to a large class of magnetically ordered states. Such a state will exhibit spin-polarized counter-propagating edge modes with a gate tunable fractionally quantized longitudinal resistance.

Acknowledgements: The author would like to acknowledge discussions with C. N. Lau and Allan H. MacDonald along with E. Prodan, E. A. Henriksen and K. Yang for comments and suggestions on the manuscript. This work was partially supported by SHINES, an Energy Frontier Research Center, funded by the U.S. Department of Energy, Office of Science, Basic Energy Sciences under Award #DE-SC0012670.

* Current Address: Department of Physics, Yeshiva University, New York, NY 10016, USA

[1] C. L. Kane and E. J. Mele, Phys. Rev. Lett. **95**, 226801 (2005).

[2] B. A. Bernevig and S.-C. Zhang, Phys. Rev. Lett. **96**, 106802 (2006).

[3] M. König, S. Wiedmann, C. Brüne, A. Roth, H. Buhmann, L. W. Molenkamp, X.-L. Qi, and S.-C. Zhang, Science **318**, 766 (2007).

[4] M. Kharitonov, Phys. Rev. B **85**, 155439 (2012).

[5] A. F. Young, J. D. Sanchez-Yamagishi, B. Hunt, S. H. Choi, K. Watanabe, T. Taniguchi, R. C. Ashoori, and P. Jarillo-Herrero, Nature **505**, 528 (2014).

[6] P. Maher, C. R. Dean, A. F. Young, T. Taniguchi, K. Watanabe, K. L. Shepard, J. Hone, and P. Kim, Nat Phys **9**, 154 (2013).

[7] M. Levin and A. Stern, Phys. Rev. Lett. **103**, 196803 (2009).

[8] E. A. Henriksen, D. Nandi, and J. P. Eisenstein, Phys. Rev. X **2**, 011004 (2012).

[9] M. Koshino and E. McCann, Phys. Rev. B **81**, 115315 (2010).

[10] S. Latil and L. Henrard, Phys. Rev. Lett. **97**, 036803 (2006).

[11] F. Guinea, A. H. Castro Neto, and N. M. R. Peres, Phys. Rev. B **73**, 245426 (2006).

[12] H. Min and A. H. MacDonald, Phys. Rev. B **77**, 155416 (2008).

[13] M. Serbyn and D. A. Abanin, Phys. Rev. B **87**, 115422 (2013).

[14] P. Stepanov, Y. Barlas, T. Espiritu, S. Che, K. Watanabe, T. Taniguchi, D. Smirnov, and C. N. Lau, Phys. Rev. Lett. **117**, 076807 (2016).

[15] To keep the discussion simple, we express $\mathcal{H}_+$ within second order perturbation theory.

[16] E. McCann and V. I. Fal'ko, Phys. Rev. Lett. **96**, 086805 (2006).

[17] Coulomb interactions lead to $n = 0$ LL orbital polarization for a partially filled zeroth LL in bilayer graphene, see Y. Barlas *et. al.*, Phys. Rev. Lett. **101**, 097601 (2008).

[18] C. N. Lau (private communication).

[19] R. B. Laughlin, Phys. Rev. Lett. **50**, 1395 (1983).

[20] F. D. M. Haldane, Phys. Rev. Lett. **51**, 605 (1983).

[21] S. A. Trugman and S. Kivelson, Phys. Rev. B **31**, 5280 (1985).

[22] Interaction induced mixing with higher LLs will lead to positive/negative self-energy corrections to the electron-like/hole-like LLs resulting in a reduction of the single-particle gap $\tilde{\Delta}$.

[23] M. R. Peterson and C. Nayak, Phys. Rev. Lett. **113**, 086401 (2014).

[24] Y. Barlas (in preparation).

[25] See Supplemental Section [url] for the derivation, which includes Refs. 26–29, and 32.

[26] S. M. Girvin and A. H. MacDonald, Phys. Rev. Lett. **58**, 1252 (1987).

[27] N. Read, Phys. Rev. Lett. **62**, 86 (1989).

[28] S. C. Zhang, T. H. Hansson, and S. Kivelson, Phys. Rev. Lett. **62**, 82 (1989).

[29] X. G. Wen and Q. Niu, Phys. Rev. B **41**, 9377 (1990).

[30] X. G. Wen, Phys. Rev. B **41**, 12838 (1990).

[31] C. L. Kane and M. P. A. Fisher, in *Perspectives in Quantum Hall Effects*, edited by S. D. Sarma and A. Pinzuk (John Wiley and Sons, John Wiley and Sons, 1997) Chap. 4, pp. 109–157.

[32] D.-H. Lee and S.-C. Zhang, Phys. Rev. Lett. **66**, 1220 (1991).